Front. Chem. China 2011, 6(1): 9–14
DOI 10.1007/s11458-011-0222-0

RESEARCH ARTICLE

Preparation and *in vitro* cytotoxicity study of poly (aspartic acid) stabilized magnetic nanoparticles

Peng YANG, Wei CHEN and Changchun WANG (✉)

Biocompatible magnetic nanoparticles were prepared by co-precipitation method in the presence of poly (aspartic acid) (PAsp) as stabilizer, which was one of the most extensively studied and used poly(amino acids). As a biocompatible dispersant, PAsp was successfully attached to the Fe_3O_4 nanoparticles, which was approved by Fourier transform infrared spectroscopy (FTIR), transmission electron microscopy (TEM) and thermogravimetric analysis (TGA). From X-ray diffraction (XRD) and vibrating sample magnetometry (VSM) measurement results, it was found that PAsp stabilized iron oxide nanoparticles possess excellent Fe_3O_4 crystal structure and superparamagnetic property. Compared with trisodium citrate stabilized magnetic nanoparticles, PAsp stabilized magnetic nanoparticles were biocompatible and with lower cytotoxicity, which makes it more applicable in medicine, biology and biomaterial science.

Keywords poly(aspartic acid) (PAsp), magnetic nanoparticles, biocompatible, *in vitro*, cytotoxicity

1 Introduction

Biocompatible superparamagnetic iron oxide nanoparticles have attracted great interests in many different fields, such as magnetic resonance imaging contrast enhancement [1,2], tissue-specific release of therapeutic agents [3], and hyperthermia [4]. Typically, magnetic iron oxide nanoparticles can be synthesized through the co-precipitation of Fe(II) and Fe(III) salts by addition of base. However, the nanoparticles of ferrofluid is likely to agglomerate and precipitate easily without stable agent. To prepare stable ferrofluid, various saturated and unsaturated fatty acids as primary and secondary surfactants were used to produce stable aqueous magnetic fluids [5–9]. However, the ferrofluid prepared by these methods was not stable enough when being diluted or severely restricted by pH variety. Recently, polymers and polymer templates were widely used as steric stabilizers for magnetic nanoparticle preparation [9–11]. In fact, the polymer stabilizers were often designed with functional groups, such as carboxyl, hydroxyl groups, which could be bound to the surface of Fe_3O_4 nanoparticles by the interaction between O and Fe atoms.

As we know, amino acid homopolymers exhibit interesting biochemical properties. Studies have shown its hormonal and enzyme-like activity and inhibition of nephrotoxicity caused by antibiotics and enhanced efficacy of cis-platinum complexes against carcinomas [12]. Poly(aspartic acid) (PAsp), as one of the typical poly(amino acid), is a water-soluble, biocompatible and biodegradable polymer and is often expected as a substitute for the conventional non-biodegradable polymers, such as poly(acrylic acid), which has been investigated as an aqueous stabilizer of iron oxide nanoparticles [13,14]. It was reported that the abundant carboxyl groups in poly(acrylic acid) could be attached to the surface of Fe atom by chemical interaction, but the cytotoxicity effect of poly(acrylic acid) was not considered, which may affect the bio-application of the ferrofluid. Moreover, genotoxicity and inflammatory have been investigated in mice treated with magnetite nanoparticles surface coated with PAsp [15], but the preparation and related properties were not illuminated.

In this paper, biocompatible superparamagnetic PAsp stabilized Fe_3O_4 nanoparticles were fabricated through the co-precipitation process in the presence of PAsp. The successful attachment of PAsp to iron oxide nanoparticles was validated by FTIR and TGA measurement. The morphology of the nanoparticles was observed by transmission electron microscopy (TEM). The crystal structure and superparamagnetic property of Fe_3O_4 was confirmed by X-ray diffraction (XRD) and vibrating sample magnetometry (VSM) analysis. Finally, the biocompatibility of PAsp stabilized magnetite nanoparticles was investigated with cytotoxicity experiment.

2 Experimental

2.1 Materials

L-aspartic acid was purchased from Shanghai Biochemical Reagent Co. Fe(II) chloride tetrahydrate was purchased from Fluka and used without further purification. Fe(III) chloride hexahydrate was purchased from ACROS and used without

Received September 30, 2010; accepted November 9, 2010
Key Laboratory of Molecular Engineering of Polymers (Ministry of Education), Department of Macromolecular Science, and Laboratory of Advanced Materials, Fudan University, Shanghai 200433, China
E-mail: ccwang@fudan.edu.cn

further purification. Sodium hydroxide was used as received. N,N-dimethylformamide (DMF) was distilled and dried via 4A molecular sieve before use. All the water used was distilled and deionized.

2.2 Synthesis of polysuccinimide (PSI)

L-aspartic acid (30.0 g, 0.22 mol) and phosphoric acid (3.3 g, 29 mmol) were mixed in a three-neck round-bottomed flask and stirred under reduced pressure at 200°C for 2 h. Then, the reaction mixture was cooled and dissolved in DMF. The solution was precipitated in excessive water and the precipitate was washed with water to get rid of the phosphoric acid. The final product was dried at 80°C under vacuum.

2.3 Hydrolysis of PSI

PSI (2.0 g) was dispersed in 10 mL deionized water and the solutions were stirred at room temperature for 1 h. Then, 2 mL of 12.5 $mol \cdot L^{-1}$ NaOH water solution were dropped into the water solution. The mixture was stirred at room temperature for another 3 h until the mixture became completely transparent. The product was dialyzed (MWCO 3,500) against deionized water for 24 h until the pH of the product solution was about 7.0 and then was lyophilized to obtain PAsp.

2.4 Synthesis of ferrofluid coated with PAsp

The stable Fe_3O_4 ferrofluid was synthesized using the method of co-precipitation of Fe(II) and Fe(III) salts in the presence of PAsp. In this process, 100 mg PAsp, 220 mg $FeCl_3 \cdot 6H_2O$ and 83.4 mg $FeCl_2 \cdot 4H_2O$ were dissolved in 50 mL water with vigorous stirring at room temperature under N_2 for 30 min. Then, 2 mL of 5 $mol \cdot L^{-1}$ NaOH water solution were slowly added to the reactor and stirring was continued for another 2 h. As the sodium hydroxide solution was added into the reactor, the color of the mixture turned from orange to brown and finally to black step by step. Then, the temperature was enhanced to 90°C and heated further for 5 h followed by stirring overnight at room temperature. The final mixture was dialyzed (MWCO 14,000) against deionic water and was partly lyophilized to obtain brown powder.

2.5 Cytotoxicity

The dialyzed ferrofluid solution was diluted to 0.5 and 0.1 mg/mL, respectively, and the Fe_3O_4 nanoparticles dispersion stabilized by trisodium citrate (the preparation method was described in Ref. [16]) was diluted to the same concentration of 0.5 and 0.1 mg/mL. Specifically, 100 μL of C2C12 cells were seeded in a 96-well flat culture plate at a density of 1×10^4 cells per well and subsequently incubated for 24 h to allow for attachment. Then, samples with different drug concentrations (0.1 and 0.5 mg/mL) were added to each group (three wells) for 24 h. A 20 μL MTT solution (5 mg/mL in PBS) was added to the wells and incubated for 4 h. MTT internalization was terminated by aspiration of the media, and the cells were lysed with 200 μL dimethyl sulfoxide (DMSO). The absorbance of the suspension was measured at 490 nm on an ELISA reader. Cell viability was calculated by means of the following formula:

$$\text{cell viability}(\%) = \frac{OD_{490(\text{sample})} - OD_{490(\text{blank})}}{OD_{490(\text{control})} - OD_{490(\text{blank})}} \times 100\%$$

2.6 Characterization

Gel permeation chromatography (GPC). GPC measurements were carried out using an HP series 1100 chromatograph equipped with Zorbax columns and RI/UV dual-mode detectors. The elution solution is 0.1 $mol \cdot L^{-1}$ $NaNO_3$, and the elution rate is 0.5 mL/min using standard PEG as calibration.
FTIR measurement. FTIR spectra were obtained in a transmission mode on a Magna 550 spectrophotometer. The ferrofluid was lyophilized to form PAsp stabilized Fe_3O_4 particles. The sample of PAsp and PAsp stabilized Fe_3O_4 particles were grounded with KBr and then compressed into pellets. The transmission spectra were obtained for 64 scans at a resolution of 8 cm^{-1}.
TEM measurement. The average particle size, size distribution, and morphology of the samples were studied using a JEM-2010F TEM. A drop of well-dispersed nanoparticle dispersion was placed onto the amorphous carbon-coated copper grid, and the sample was dried at ambient temperature before loaded into the microscope.
XRD measurement. The crystal structure of the iron oxide nanoparticles stabilized by PAsp was obtained by the powder XRD pattern of each sample recorded with Rigaku/Japan diffractometer using a monochromatized X-ray beam with nickel-filtered Cu Kα radiation with 4°/min scan rate. A continuous scan mode was used to collect 2θ data from 20° to 75°.
Magnetic measurements. The magnetization of the PAsp stabilized nanoparticles was measured as a function of the applied magnetic field H with a Ppms-9T-evercool VSM superconducting quantum interference device magnetometer.

3 Results and discussion

3.1 Synthesis of PAsp and ferrofluid

PSI was synthesized by thermal polymerization of aspartic acid monomer. The final product of PAsp was obtained by hydrolyzing PSI with sodium hydroxide. Due to the two

reactive sites for the hydrolysis, the obtained product was actually a mixture of two isomers, including α and β structure, the α subunit is the standard protein unit. The synthesis process was summarized in Scheme 1. The GPC measurement was carried out in 0.1 mol·L^{-1} $NaNO_3$ solution and the molecular weight of PAsp was determined to be about 1.0×10^4 (Mn).

Conventionally, the Fe_3O_4 nanoparticles are prepared by adding base to an aqueous solution of Fe^{2+} and Fe^{3+}. The overall reaction can be written as follows [17]:

$$Fe^{2+} + 2Fe^{3+} + 8OH^- \rightleftharpoons Fe(OH)_2 + 2Fe(OH)_3 \rightarrow Fe_3O_4 + 4H_2O \quad (1)$$

However, the pure Fe_3O_4 nanoparticles synthesized by the conventional method can aggregate easily. To prevent the aggregation, Fe_3O_4 nanoparticles produced by reaction (1) were usually coated with low molecular weight or polymer stabilizers. The low molecular weight steric stabilizers for magnetic fluids usually contain a complexing group that has strong coordination ability to the iron atom of the magnetic particles. These complexing groups include carboxylic acids [5], thiols [18], and phosphonic acids [19]. In the design of polymer stabilizers, these complexing groups, such as carboxylic acids, have also been chosen in order to get stable ferrofluids, which have been reported to chemisorb onto magnetite surface through reaction with iron on the particle surface [20].

In our experiments, stable aqueous iron oxide nanoparticles dispersions were obtained by co-precipitation of ferrous (Fe^{2+}) and ferric (Fe^{3+}) solution in the presence of water-soluble and biocompatible PAsp. The biocompatible polypeptide PAsp was successfully bonded to the surface of Fe_3O_4 nanoparticles through the attachment of carboxyl groups to the surface of the particles and the stable ferrofluid was formed. The ferrofluid could be suspended homogeneously and stably in water. The morphology of the magnetic nanoparticles is shown in Fig. 1.

3.2 FTIR analysis

To corroborate the successful attachment of PAsp onto the surface of iron oxide nanoparticles, the FTIR spectra of pure

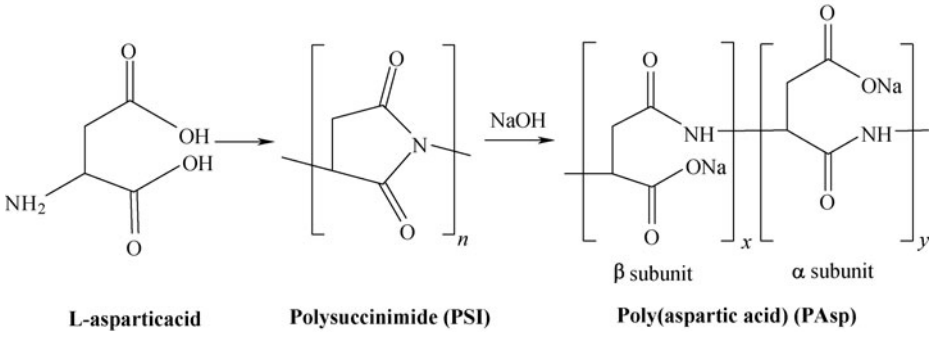

Scheme 1 The synthesis scheme of PAsp from aspartic acid

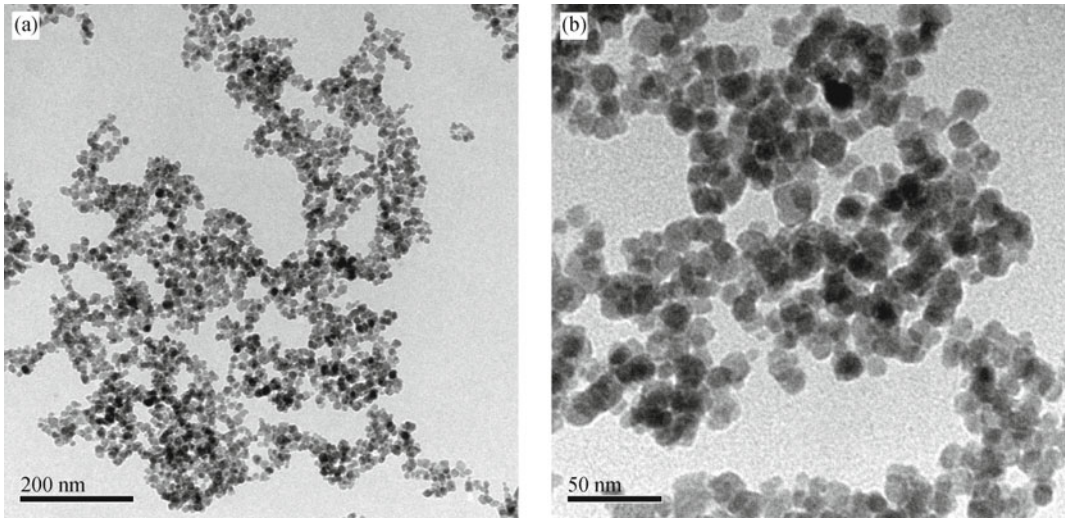

Figure 1 TEM images of iron oxide nanoparticles stabilized with PAsp

Fe_3O_4, PAsp and PAsp stabilized Fe_3O_4 were recorded, and the results are listed in Fig. 2. The peaks at 1,650, 1,600 and 1,540 cm^{-1} were attributed to the carboxyl group stretch and N-H vibration of amide of PAsp in Fig. 2(a) and (b). A new band at 1,592 cm^{-1}, which is characteristic adsorption of COO^- onto the surface of Fe_3O_4 nanoparticles [21] did not appear as clearly as usual because of the strong amide N-H vibration absorption bond at 1,600 cm^{-1}. The peak at 1,400 cm^{-1} was attributed to the stretch of C-O. A comparison of Fig. 2(b) and (c) showed that the wave numbers located at 580 and 434 cm^{-1} were the characteristic absorption bands of the Fe-O bond [22], suggesting the formation of Fe_3O_4 nanoparticles. The new bonds in 1,400, 1,540, 1,600 and 1,650 cm^{-1} indicated that PAsp was successfully attached to the iron oxide nanoparticles.

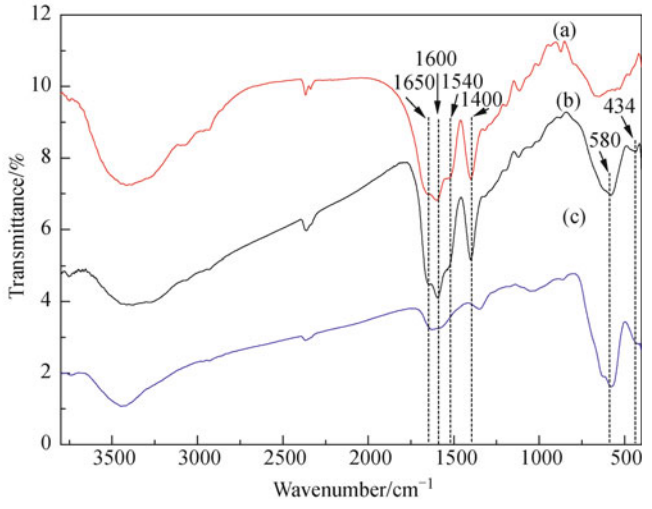

Figure 2 FTIR spectra of (a) PAsp, (b) PAsp stabilized Fe_3O_4 and (c) pure Fe_3O_4

3.3 XRD analysis

The effect of PAsp on the preparation of Fe_3O_4 was investigated through XRD analysis of pure Fe_3O_4 and PAsp stabilized Fe_3O_4 (Fig. 3). Six characteristic peaks for Fe_3O_4 at 2θ = 30.2°, 35.7°, 43.4°, 53.7° and 62.9° were observed for both samples, which were consistent with the standard data for magnetite [23]. Besides the magnetite peaks, we did not observe any other peak in the diffraction pattern in the PAsp stabilized Fe_3O_4 sample, which suggests the good crystallinity of the iron oxide nanoparticles.

3.4 TGA analysis

Figure 4 shows the TGA analysis of the pure Fe_3O_4 nanoparticles and the ferrofluid particles synthesized in the presence of PAsp. The pure Fe_3O_4 nanoparticles showed few weight loss from 100°C to 800°C. However, there were two

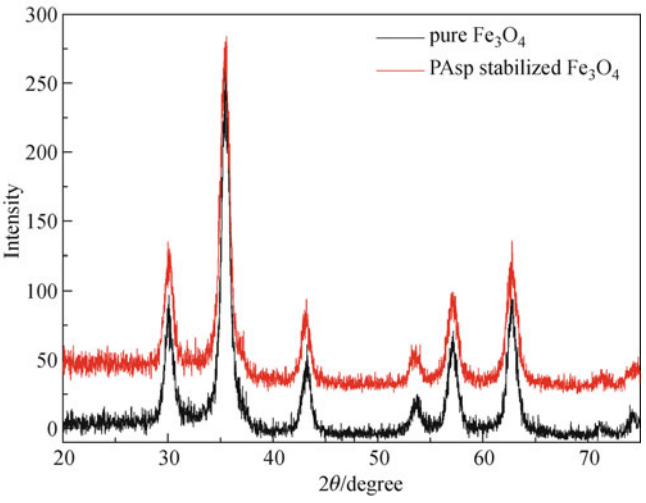

Figure 3 X-ray powder diffraction patterns of the pure Fe_3O_4 and PAsp stabilized Fe_3O_4

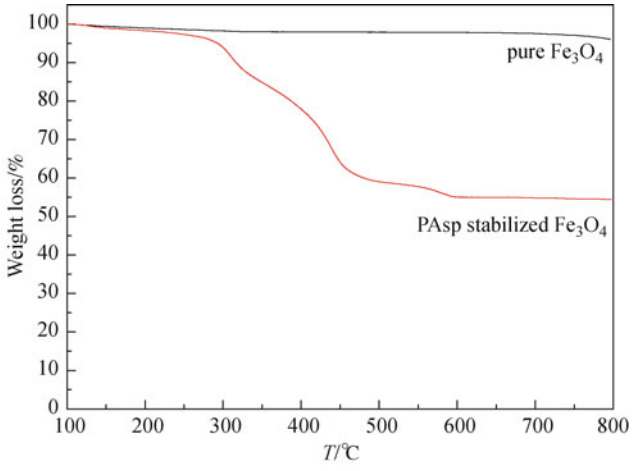

Figure 4 TGA analysis of the pure Fe_3O_4 and PAsp stabilized Fe_3O_4

main stages in the TGA curve of PAsp stabilized Fe_3O_4: When the temperature was raised to higher than 300°C (about 310°C), the weight loss was significant due to the dehydration and decarboxylation of the carboxylic acid [24]. In the second stage when the temperature was about 440°C, an obvious weight loss was derived from the degradation of PAsp. Theoretically, from the feed composition, the weight ratio of PAsp to Fe_3O_4 nanoparticles in the ferrofluid was calculated to be 1/1; on the other hand, the whole weight loss from TGA curve was about 45%. The result indicated that most PAsp could be stably attached to the surface of Fe_3O_4 nanoparticles and could not be removed during the dialysis process.

3.5 Magnetic property

The superparamagnetic property of Fe_3O_4 nanoparticles was usually investigated with VSM. The curve of magnetite

specific magnetization versus applied field is shown in Fig. 5. From the result, it can be found that the PAsp stabilized Fe_3O_4 nanoparticles possess superparamagnetic behavior with high magnetic susceptibility, and the coercivity and remanence were almost immeasurable. The magnetite content of this sample was 55% from TGA analysis; thus, the normalized saturation magnetization value was about 45 emu/g, which was much lower than that of bulk magnetite (92 emu/g) [11]. The decrease of the saturation magnetization was due to the successful attachment of PAsp to the surface of nanoparticles.

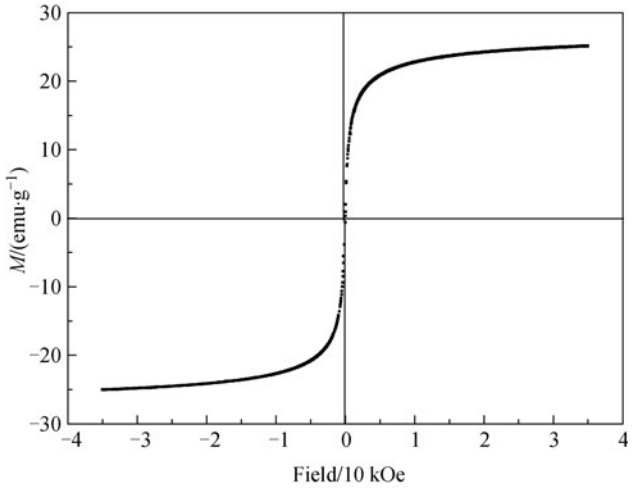

Figure 5 SQUID magnetization curve of PAsp stabilized Fe_3O_4 nanoparticles

3.6 Measurement of the *in vitro* cytotoxicity

To test the biocompatibility and cytotoxicity of PAsp stabilized magnetic nanoparticles, trisodium citrate stabilized magnetic nanoparticles were used in comparison of samples instead of pure Fe_3O_4 nanoparticles, because the iron oxide particles without surface modification agglomerate easily and form large clusters in a short period, which is not suitable for cytotoxicity measurement. As shown in Fig. 6, when the cells were cultured in medium containing 0.1 mg/mL magnetic nanoparticles, the viability of both samples remained at $> 90\%$ in the first day, but on the second day, the viability of trisodium citrate stabilized nanoparticles decreased to 67%, which indicated that trisodium citrate stabilized nanoparticles imparted cytotoxicity effects to cells after 2 days of incubation. Meanwhile, the viability of cells cultured in medium containing PAsp stabilized magnetic nanoparticles did not diminish. When the concentration of the ferrofluids was increased to 0.5 mg/mL, the viability of the cells cultured in medium containing PAsp stabilized nanoparticles did not change significantly after 1 or 2 days compared with that at the concentration of 0.1 mg/mL (Fig. 7). However, the viability of

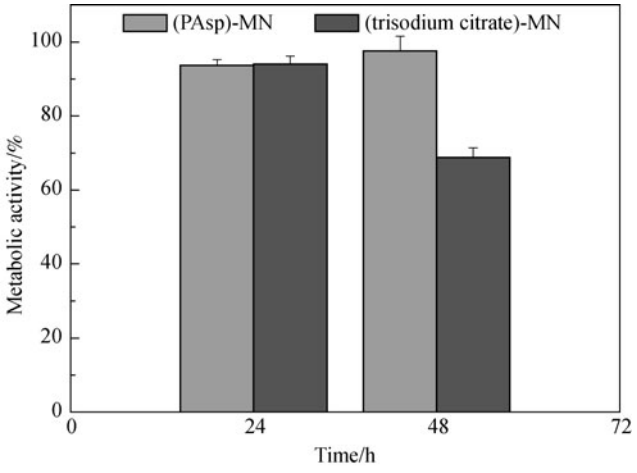

Figure 6 Viability of C2C12 cells cultured in medium containing 0.1 mg/mL magnetic nanoparticles

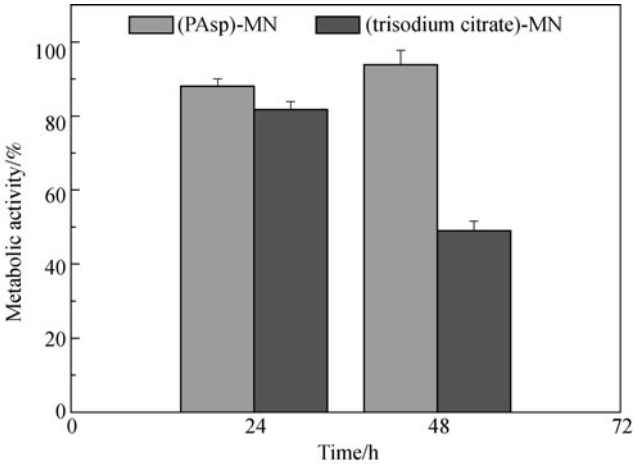

Figure 7 Viability of C2C12 cells cultured in medium containing 0.5 mg/mL magnetic nanoparticles

the sample stabilized by trisodium citrate decreased obviously because the nanoparticles imparted more cytotoxicity effects to cells as the concentration increased.

From the above experiment, we can conclude that the PAsp stabilized iron oxide nanoparticles exhibited good biocompatibility and low cytotoxicity, which could have an extensive application in biological area and drug delivery system.

4 Conclusion

In summary, co-precipitation of ferrous (Fe^{2+}) and ferric (Fe^{3+}) salts in a base solution in the presence of PAsp was conducted to fabricate a stable biocompatible magnetic nanoparticle dispersion. The stable and biocompatible properties of Fe_3O_4 nanoparticles originate from the abundant carboxyl groups of PAsp and inherent biocompatible feature of poly(amino acid).

A big amount of PAsp was attached to the surface of magnetic nanoparticles, which was proven by FTIR, TEM and TGA. The biocompatibility and low cytotoxicity of these nanoparticles were demonstrated by MTT experiments.

Acknowledgements This work was supported by the National Natural Science Foundation of China (Grant Nos. 20974023, 21034003 and 51073040) and Shanghai Committee of Science and Technology, China (Grant No. 10XD1400500).

References

1. Lévy, M.; Lagarde, F.; Maraloiu, V. A.; Blanchin, M. G.; Gendron, F.; Wilhelm, C.; Gazeau, F., *Nanotechnology* **2010**, *21*, 395103
2. Chen, D. Y.; Li, N. J.; Gu, H. W.; Xia, X. W.; Xu, Q. F.; Ge, J. F.; Lu, J. M.; Li, Y. G., *Chem. Commun.* **2010**, *46*, 6708–6710
3. Gupta, P. K.; Hung, C. T., *Science* **1989**, *44*, 175
4. Chan, D. C. F.; Kirpotin, D.; Bunn, P. A., *J. Magn. Magn. Mater*. **1993**, *122*, 374–378
5. Shen, L.; Laibinis, P. E.; Hatton, T. A., *Langmuir* **1999**, *15*, 447–453
6. Shen, L.; Stachowiak, A.; Hatton, A.; Laibinis, P. E., *Langmuir* **2000**, *16*, 9907–9911
7. Wang, P. C.; Chiu, W. Y.; Lee, C. F.; Young, T. H., *J. Polym. Sci. A Polym. Chem*. **2004**, *42*, 5695–5705
8. Wormuth, K., *J. Colloid Interface Sci*. **2001**, *241*, 366–377
9. Harris, L. A.; Goff, J. D.; Carmichael, A. Y.; Riffle, J. S.; Harburn, J. J.; Saunders, M., *Chem. Mater*. **2003**, *15*, 1367
10. Wan, S. R.; Huang, J. S.; Yan, H. S.; Liu, K. L., *J. Mater. Chem*. **2006**, *16*, 298
11. Thünemann, A. F.; Schütt, D.; Kaufner, L.; Pison, U.; Möhwald, H., *Langmuir* **2006**, *22*, 2351–2357
12. Wolk, S. K.; Swift, G.; Paik, Y. H.; Yocom, K. M.; Smith, R. L.; Simon, E. S., *Macromolecular* **1994**, *27*, 7613–7620
13. Lin, Y. J.; Wang, L.; Lin, J. G.; Hung, Y. Y.; Chiu, W. Y., *Synth. Met*. **2003**, *135*, 769–770
14. Lin, C. L.; Lee, C. F.; Chiu, W. Y., *J. Colloid Interface Sci*. **2005**, *291*, 411–420
15. Sadeghiania, N.; Barbosaa, L. S.; Silvaa, L. P.; Azevedoa, R. B.; Moraisb, P. C.; Lacava, Z. G. M., *J. Magn. Magn. Mater*. **2005**, *289*, 466–468
16. Guo, J.; Yang, W. L.; Deng, Y. H.; Wang, C. C.; Fu, S. K., *Small* **2005**, *1*, 737–743
17. Gupta, A. K.; Gupta, M., *Biomaterials* **2005**, *26*, 3995–4021
18. Fauconnier, N.; Pons, J. N.; Roger, J.; Bee, A., *J. Colloid Interface Sci*. **1997**, *194*, 427–433
19. Portet, D.; Denizot, B.; Rump, E.; Lejeune, J. J.; Jallet, P., *J. Colloid Interface Sci*. **2001**, *238*, 37–42
20. Cornell, R. M.; Schertmann, U., The Iron Oxides: Structure, Properties, Reactions, Occurrence and Uses VCH Publishers: Weinheim, 1996
21. Wan, S. R.; Zheng, Y.; Liu, Y. Q.; Yan, H. S.; Liu, K. L., *J. Mater. Chem*. **2005**, *15*, 3424
22. Ma, M.; Zhang, Y.; Yu, W.; Shen, H. Y.; Zhang, H. Q.; Gu, N., *Colloids Surf. A Physicochem. Eng. Asp*. **2003**, *212*, 219–226
23. Zhou, Z. H.; Wang, J.; Liu, X.; Chan, H. S. O., *J. Mater. Chem*. **2001**, *11*, 1704–1709
24. Fyfe, C. A.; McKinnon, M. S., *Macromolecules* **1986**, *19*, 1909–1912